Biomedical Optics EXPRESS

Optical fiber LPG biosensor integrated microfluidic chip for ultrasensitive glucose detection

Ming-jie Yin,[1] Bobo Huang,[1,2] Shaorui Gao,[1] A. Ping Zhang,[1,*] and Xuesong Ye[2]

[1]*Photonics Research Center, Department of Electrical Engineering, The Hong Kong Polytechnic University, Kowloon, Hong Kong SAR, China*

[2]*Biosensor National Special Laboratory, College of Biomedical Engineering and Instrument Science, Zhejiang University, Hangzhou 310027, China*

[*]*azhang@polyu.edu.hk*

Abstract: An optical fiber sensor integrated microfluidic chip is presented for ultrasensitive detection of glucose. A long-period grating (LPG) inscribed in a small-diameter single-mode fiber (SDSMF) is employed as an optical refractive-index (RI) sensor. With the layer-by-layer (LbL) self-assembly technique, poly (ethylenimine) (PEI) and poly (acrylic acid) (PAA) multilayer film is deposited on the SDSMF-LPG sensor for both supporting and signal enhancement, and then a glucose oxidase (GOD) layer is immobilized on the outer layer for glucose sensing. A microfluidic chip for glucose detection is fabricated after embedding the SDSMF-LPG biosensor into the microchannel of the chip. Experimental results reveal that the SDSMF-LPG biosensor based on such a hybrid sensing film can ultrasensitively detect glucose concentration as low as 1 nM. After integration into the microfluidic chip, the detection range of the sensor is extended from 2 μM to 10 μM, and the response time is remarkablely shortened from 6 minutes to 70 seconds.

OCIS codes: (060.2370) Fiber optics sensors; (050.2770) Gratings; (160.1435) Biomaterials; (280.1415) Biological sensing and sensors.

References and links

1. J. Wang, "Electrochemical glucose biosensors," Chem. Rev. **108**(2), 814–825 (2008).
2. S. K. Vashist, D. Zheng, K. Al-Rubeaan, J. H. T. Luong, and F.-S. Sheu, "Technology behind commercial devices for blood glucose monitoring in diabetes management: A review," Anal. Chim. Acta **703**(2), 124–136 (2011).
3. L. C. Clark, Jr. and C. Lyons, "Electrode systems for continuous monitoring in cardiovascular surgery," Ann. N. Y. Acad. Sci. **102**(1), 29–45 (1962).
4. S. Brahim, D. Narinesingh, and A. Guiseppi-Elie, "Polypyrrole-hydrogel composites for the construction of clinically important biosensors," Biosens. Bioelectron. **17**(1-2), 53–59 (2002).
5. X. Kang, J. Wang, H. Wu, I. A. Aksay, J. Liu, and Y. Lin, "Glucose oxidase-graphene-chitosan modified electrode for direct electrochemistry and glucose sensing," Biosens. Bioelectron. **25**(4), 901–905 (2009).
6. H.-F. Cui, K. Zhang, Y.-F. Zhang, Y.-L. Sun, J. Wang, W.-D. Zhang, and J. H. T. Luong, "Immobilization of glucose oxidase into a nanoporous TiO_2 film layered on metallophthalocyanine modified vertically-aligned carbon nanotubes for efficient direct electron transfer," Biosens. Bioelectron. **46**, 113–118 (2013).
7. G. M. Whitesides, "The origins and the future of microfluidics," Nature **442**(7101), 368–373 (2006).
8. D. Janasek, J. Franzke, and A. Manz, "Scaling and the design of miniaturized chemical-analysis systems," Nature **442**(7101), 374–380 (2006).
9. R. G. Blazej, P. Kumaresan, and R. A. Mathies, "Microfabricated bioprocessor for integrated nanoliter-scale Sanger DNA sequencing," Proc. Natl. Acad. Sci. U.S.A. **103**(19), 7240–7245 (2006).
10. P. Labroo and Y. Cui, "Graphene nano-ink biosensor arrays on a microfluidic paper for multiplexed detection of metabolites," Anal. Chim. Acta **813**, 90–96 (2014).
11. Y.-H. Lin, S.-H. Wang, M.-H. Wu, T.-M. Pan, C.-S. Lai, J.-D. Luo, and C.-C. Chiou, "Integrating solid-state sensor and microfluidic devices for glucose, urea and creatinine detection based on enzyme-carrying alginate microbeads," Biosens. Bioelectron. **43**, 328–335 (2013).
12. M. M. Picher, S. Küpcü, C.-J. Huang, J. Dostalek, D. Pum, U. B. Sleytr, and P. Ertl, "Nanobiotechnology advanced antifouling surfaces for the continuous electrochemical monitoring of glucose in whole blood using a lab-on-a-chip," Lab Chip **13**(9), 1780–1789 (2013).

#259792 Received 22 Feb 2016; revised 27 Mar 2016; accepted 27 Mar 2016; published 28 Apr 2016

13. Y. Wang, Q. He, Y. Dong, and H. Chen, "In-channel modification of biosensor electrodes integrated on a polycarbonate microfluidic chip for micro flow-injection amperometric determination of glucose," Sens. Actuators B Chem. **145**(1), 553–560 (2010).
14. F. Baldini, M. Brenci, F. Chiavaioli, A. Giannetti, and C. Trono, "Optical fibre gratings as tools for chemical and biochemical sensing," Anal. Bioanal. Chem. **402**(1), 109–116 (2012).
15. A. Deep, U. Tiwari, P. Kumar, V. Mishra, S. C. Jain, N. Singh, P. Kapur, and L. M. Bharadwaj, "Immobilization of enzyme on long period grating fibers for sensitive glucose detection," Biosens. Bioelectron. **33**(1), 190–195 (2012).
16. R.-Z. Yang, W.-F. Dong, X. Meng, X.-L. Zhang, Y.-L. Sun, Y.-W. Hao, J.-C. Guo, W.-Y. Zhang, Y.-S. Yu, J.-F. Song, Z.-M. Qi, and H.-B. Sun, "Nanoporous TiO_2/polyion thin-film-coated long-period grating sensors for the direct measurement of low-molecular-weight analytes," Langmuir **28**(23), 8814–8821 (2012).
17. B. Luo, Z. Yan, Z. Sun, Y. Liu, M. Zhao, and L. Zhang, "Biosensor based on excessively tilted fiber grating in thin-cladding optical fiber for sensitive and selective detection of low glucose concentration," Opt. Express **23**(25), 32429–32440 (2015).
18. V. Bhatia and A. M. Vengsarkar, "Optical fiber long-period grating sensors," Opt. Lett. **21**(9), 692–694 (1996).
19. S. W. James and R. P. Tatam, "Optical fibre long-period grating sensors: characteristics and application," Meas. Sci. Technol. **14**(5), R49–R61 (2003).
20. J. H. Chong, P. Shum, H. Haryono, A. Yohana, M. K. Rao, C. Lu, and Y. Zhu, "Measurements of refractive index sensitivity using long-period grating refractometer," Opt. Commun. **229**(1–6), 65–69 (2004).
21. Z. Yan, Z. Sun, K. Zhou, B. Luo, J. Li, H. Wang, Y. Wang, W. Zhao, and L. Zhang, "Numerical and experimental analysis of sensitivity-enhanced ri sensor based on ex-tfg in thin cladding fiber," J. Lightwave Technol. **33**(14), 3023–3027 (2015).
22. M. J. Yin, C. Wu, L. Y. Shao, W. K. E. Chan, A. P. Zhang, C. Lu, and H. Y. Tam, "Label-free, disposable fiber-optic biosensors for DNA hybridization detection," Analyst (Lond.) **138**(7), 1988–1994 (2013).
23. Y.-H. Yang, M. Haile, Y. T. Park, F. A. Malek, and J. C. Grunlan, "Super gas barrier of all-polymer multilayer thin films," Macromolecules **44**(6), 1450–1459 (2011).
24. M. J. Yin, B. B. Gu, J. W. Qian, A. P. Zhang, Q. F. An, and S. L. He, "Highly sensitive and selective fiber-optic modal interferometric sensor for detecting trace mercury ion in aqueous solution," Anal. Methods **4**(5), 1292–1297 (2012).
25. I. Tokarev, I. Tokareva, V. Gopishetty, E. Katz, and S. Minko, "Specific biochemical-to-optical signal transduction by responsive thin hydrogel films loaded with noble metal nanoparticles," Adv. Mater. **22**(12), 1412–1416 (2010).
26. M. Yin, B. Gu, Q. Zhao, J. Qian, A. Zhang, Q. An, and S. He, "Highly sensitive and fast responsive fiber-optic modal interferometric pH sensor based on polyelectrolyte complex and polyelectrolyte self-assembled nanocoating," Anal. Bioanal. Chem. **399**(10), 3623–3631 (2011).
27. Q. Zhao, M. Yin, A. P. Zhang, S. Prescher, M. Antonietti, and J. Yuan, "Hierarchically structured nanoporous poly(ionic liquid) membranes: Facile preparation and application in fiber-optic pH sensing," J. Am. Chem. Soc. **135**(15), 5549–5552 (2013).
28. P. N. Nge, C. I. Rogers, and A. T. Woolley, "Advances in microfluidic materials, functions, integration, and applications," Chem. Rev. **113**(4), 2550–2583 (2013).
29. D. Buenger, F. Topuz, and J. Groll, "Hydrogels in sensing applications," Prog. Polym. Sci. **37**(12), 1678–1719 (2012).
30. P. A. Palod and V. Singh, "Improvement in glucose biosensing response of electrochemically grown polypyrrole nanotubes by incorporating crosslinked glucose oxidase," Mater. Sci. Eng. C **55**, 420–430 (2015).
31. X. Wang, F. Liu, X. Zheng, and J. Sun, "Water-enabled self-healing of polyelectrolyte multilayer coatings," Angew. Chem. Int. Ed. Engl. **50**(48), 11378–11381 (2011).
32. Y.-A. Yang and C.-H. Lin, "Multiple enzyme-doped thread-based microfluidic system for blood urea nitrogen and glucose detection in human whole blood," Biomicrofluidics **9**(2), 022402 (2015).

1. Introduction

Highly sensitive and rapid detection of glucose content has become one of essential biomedical diagnostic technologies. For instance, two main causes of diabetes mellitus are insulin deficiency and hyperglycemia in human body, and both of the two parameters can be reflected by blood glucose concentrations [1,2]. The glucose biosensor was firstly demonstrated by using electrochemical glucose enzyme electrodes [3]. Thereafter, many electronic techniques based on glucose oxidase (GOD) have been proposed for glucose biosensor development [4–6]. For example, the conductive polypyrrole encapsulated by pHEMA hydrogel was adopted as matrix for GOD, which was then deposited on Pt electrode for glucose detection [4]; GOD-graphene-chitosan nanocomposite was demonstrated as active component and glassy carbon was used as electrode for glucose biosensor fabrication [5]. However, the electron transfer between GOD and electrode is not efficient. Moreover, those glucose biosensors are usually too bulky and costly for daily use and their sample consumption is relatively high.

#259792 Received 22 Feb 2016; revised 27 Mar 2016; accepted 27 Mar 2016; published 28 Apr 2016

One of potential solutions to these problems is to use microfluidic chips due to their advantages of compactness, low-sample consumption, and low cost [7,8]. Moreover, microfluidic chip technology offers a platform to integrate sensors with functional components (e.g. microfluidic mixers) to achieve the lab-on-a-chip analysis system [9]. Recently, it was demonstrated electrochemical glucose biosensors can be integrated into microfluidic channels to develop easy-handle, low-cost, and portable microfluidic chips [10–13]. However, electroactive interference problems often appear in electrochemical sensors because some endogenous reducing species (e.g. ascorbic and uric acids) and drugs (e.g., acetaminophen) are electroactive [1].

The limitation can be overcome by using optical fiber sensor technology due to its well-known immunity to electromagnetic interferences [14–16]. For instance, Tiwari et al. [15] adopted GOD immobilized long-period grating (LPG) sensor for detection of glucose; Yang et al. [16] proposed a nanoporous TiO_2/polyion film coated LPG sensor to improve the detection limitation (~10^{-7} M); Luo et al. [17] suggested GOD modified tilted fiber grating sensor for highly sensitive detection of low glucose concentraion. Therefore, a promising solution is to integrate fiber-optic sensor with microfluidic technology to develop high-performance glucose sensing devices.

In this paper, we demonstrate an LPG biosensor fabricated in a small-diameter single-mode fiber (SDSMF) for glucose sensor development and on-chip integration, as shown in Fig. 1. A hybrid sensing film using multi-layer poly (ethylenimine) (PEI) and poly (acrylic acid) (PAA) supporting film and a negatively charged glucose oxidase (GOD) outer layer is deposited on the side surface of LPG for glucose sensing and signal enhancement. The SDSMF-LPG biosensor is then integrated into a microfluidic chip for fast and low-sample-consumption glucose analysis. Experimental results reveal that the fabricated LPG glucose sensor can detect ultralow concentration of glucose (~10^{-9} M). The performances of the biosensor, in terms of response time and detection range, are significantly improved after integrated into the microfluidic chip.

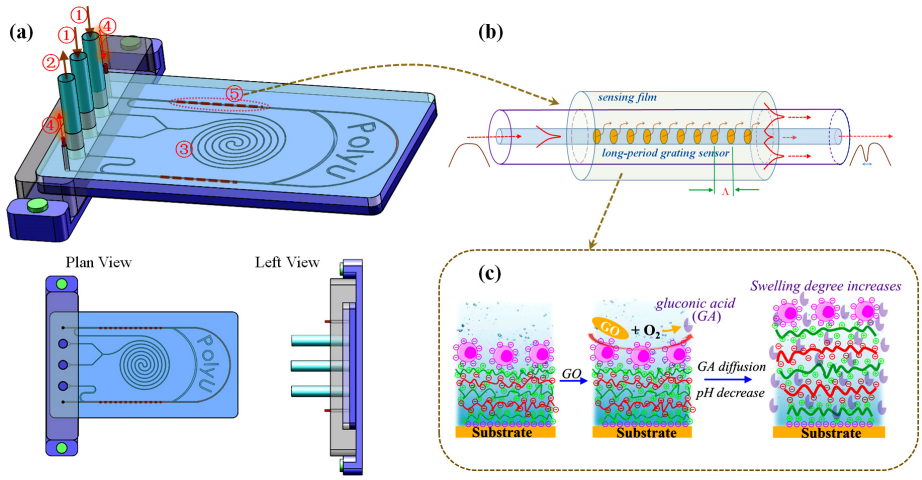

Fig. 1. (a) Schematic design of the optical fiber biosensor integrated microfluidic chip: ① are two inlets, ② is outlet, ③ is a spiral mixture, ④ are optical fibers and ⑤ is the embedded LPG sensor. (b) The mode coupling and optical resonance in the LPG biosensor. (c) Working mechanism of the multilayer film for glucose sensing and signal enhancement.

2. Materials and methods

2.1 Chemical and materials

Poly (ethylenimine) (PEI, M_w = 750 000 g mol^{-1}, 50 wt% aqueous solution), poly (acrylic acid) (PAA, M_w = 100 000 g mol^{-1}, 35 wt% aqueous solution) and glucose oxidase (GOD)

#259792 Received 22 Feb 2016; revised 27 Mar 2016; accepted 27 Mar 2016; published 28 Apr 2016

(149800 U/g) were purchased from Sigma-Aldrich Co. Ltd. (USA). Glucose anhydrous was obtained from Shenzhen Chemical Reagent Company (Shenzhen, China). EPON resin SU-8 was purchased from Momentive Performance Materials Inc. (USA). Tributylamine (TBA) and cyclopentanone were obtained from Meryer Chemical Technology Co., Ltd. (Shanghai, China). 4-Octyloxydiphenyliodonium hexafluoroantimonate (OPPI) was kindly provided by Hampford Research Inc. (USA). Silicone elastomer (SYLGARD® 184) was manufactured by Dow Corning (China) Holding Co. Ltd. All the inorganic materials ($CaCl_2$, NaCl, H_2SO_4, H_2O_2, HCl and KOH) used were analytical grade. Deionized water (DI water) with a resistance of 18 MΩ cm was used in all the experiments.

2.2 Fabrication of LPGs in small-diameter single-mode fiber (SDSMF)

A small-diameter single-mode fiber (RC1550 80-21/165, Yangtze Optical Fiber and Cable Joint Stock Limited Company, China) with the diameter of 80 μm was used for LPG fabrication. The optical fiber was initially hydrogen loaded at a pressure of 1500 psi at room temperature for one week to enhance photosensitivity. Thereafter, a point-by-point technique was utilized to fabricate LPGs using a KrF pulsed Excimer laser (BraggStar-M, Coherent Inc.) operating at the wavelength of 248 nm.

2.3 Preparation of the glucose sensing films by LbL self-assembly technique

The concentrations of both positively charged PEI and negatively charged PAA were diluted to 2.0 g/L, with the pH of 11.0 and 3.0, respectively. The concentration of negatively charged GOD was 50 mg/L at pH 7.0. The LbL electrostatic self-assembly of PEI, PAA, and GOD was carried out on silicon wafers (10mm × 10 mm) for testing and characterization and then applied on SDSMF-LPGs, respectively. The substrates were cleaned with piranha solution (7: 3 of 98% H_2SO_4 and 30% H_2O_2), washed with large volumes of DI water and dried with nitrogen to get negatively charged surface. The negatively charged substrates were then dipped into the positively charged PEI and negatively charged PAA solutions alternatively, each for 10 minutes at room temperature. The substrates were rinsed with DI water for 1 minute in between the immersions in polycation and polyanion solutions to remove the excess adsorbed components, and dried with nitrogen. The process was repeated until desired numbers of bilayers were fabricated (one bilayer consists of one PEI layer and one PAA layer and is expressed as $(PEI/PAA)_1$). The substrates were then dipped into a negatively charged GOD solution for 60 minutes, and immersed in DI water for 3 minutes, and dried with nitrogen again.

2.4 Fabrication of the microfluidic chip

EPON resin SU-8 was dissolved into cyclopentanone in the concentration of 70 wt%. 0.5 wt% TBA and 2 wt% OPPI were added into solution under stirring and fully dissolved. The solutions were firstly spin-coating on the surface of a pretreated silicon wafer (2 cm × 2 cm) at a speed of 1000 rpm. Then the substrate was soft baked at 65 and 95°C for 10 and 30 min, respectively. The designed microfluidic chip was converted into a series of image data and then loaded onto a digital micromirror device (DMD) based maskless lithography system for generation of optical patterns. UV light source (365 nm) was used for optically patterning the SU-8 photoresisit. After exposure, the substrate was post baked at 65 and 95 °C for 1 and 10 min, respectively, to selectively crosslink the exposed portions of the film. The master of designed microfluidic chip was then fabricated after a development process.

The PDMS microfluidic chip was fabricated by using moulding and thermally crosslinking method. A 10:1 mixture of PDMS and crosslinker was used for the chip fabrication. The mixture was degassed in a vacuum chamber for 30 minute. Thereafter, the PDMS mixture was poured onto the SU-8 master and cured in an oven at 75 °C for 1 hour. The PDMS slice with microfluidic channels was then peeled off from the mold and several holes were drilled by using the punch. The PDMS slice was eventually bonded upon a cover glass after treated with oxygen plasma for 3 minutes.

#259792 Received 22 Feb 2016; revised 27 Mar 2016; accepted 27 Mar 2016; published 28 Apr 2016

2.5 Biosensor tests

1 mM glucose solution was prepared by adding 0.018g glucose powder into 100 mL DI water. Glucose solutions of other concentrations, including 100 μM, 10 μM, 2 μM, 0.1 μM, 20 nM, and 1 nM, were prepared by diluting the previously prepared solution. In order to mimic the blood samples, 0.585 g NaCl was added to each glucose solution to prepare 0.1 M NaCl buffer solution.

Optical fiber LPG glucose biosensors were packaged in a shallow Teflon groove before testing. Glucose solutions with different concentrations were injected into the Teflon groove by syringe. After each test, the previously used glucose solution was extracted, and then the Teflon groove and biosensor was thoroughly flushed by using 0.1 M NaCl buffer solution.

LPG sensor integrated microfluidic chip was tested by injection of glucose solutions using a programmable syringe pump (NE-4000 Double Syringe Pump, New Era Pump Systems Inc., NY USA). Flow rate was controlled by the programmable syringe pump. A flow rate of 5 μL/min was used in the experiments.

2.6 Characterization

The thickness of multilayer film was measured by a surface profilometer (Veeco, Germany). Scanning probe microscopy (DI Nano Scope 8, Veeco, Germany) and atomic force microscopy (AFM) mode were performed on a 9146JVHC station. The silicon tips (NSG10, NT-MDT) were operated with a resonance frequency of 288 kHz. The 3D microstructures were measured by using 3D laser scanning microscope (VK-X200, KEYENCE, Japan) in a non-contact scanning manner.

3. Results and discussion

3.1 RI sensing property of SDSMF-LPGs

When an optical fiber is inscribed with an LPG structure, a resonant mode coupling between the guided core mode and a forward-propagating cladding mode can be excited at the wavelength [18,19]:

$$\lambda = [n_{eff}(\lambda) - n_{clad}^{i}(\lambda)]\Lambda \tag{1}$$

where $n_{eff}(\lambda)$ is the effective RI of the core mode at the wavelength λ, $n_{clad}^{i}(\lambda)$ is the RI of the LP_{0i} cladding mode and Λ is the period of the LPG. It can be seen from Eq. (1) that the resonant wavelength λ is determined by $n_{clad}^{i}(\lambda)$ which depends on the evanescent field of the cladding mode. Therefore, LPG is a versatile technology for label-free RI sensing.

In the experiments, a 2-cm length LPG with the period of 390 μm was inscribed in the SDSMF. The measured transmission spectrum of SDSMF-LPG is shown in Fig. 2. The spectral dip corresponding to the coupling with LP_{05} cladding mode at the wavelength of ~1510 nm is chosen for sensing due to its highest signal-to-noise ratio.

#259792 Received 22 Feb 2016; revised 27 Mar 2016; accepted 27 Mar 2016; published 28 Apr 2016

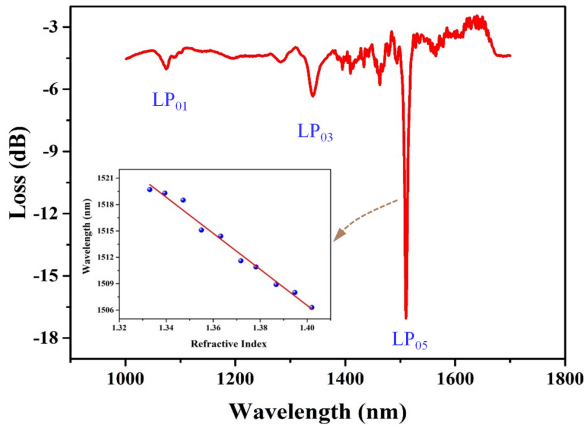

Fig. 2. Transmission spectrum of the fabricated SDSMF-LPG. The inset shows the response of its deepest spectral dip to the RI changes of surrounding medium.

Since $CaCl_2$ aqueous solutions have relatively wide range of RI values, they have been chosen to characterize the responses of the LPG sensor to RI changes. The measured results are shown in the inset of Fig. 2. One can see that the central wavelength of the spectral dip nearly linearly shifts to shorter wavelength with the increment of RI ranging from 1.33 to 1.4. The RI sensitivity deduced by linear fitting is ~205 nm/R.I.U. It is noteworthy that the RI sensitivity of the LPG is higher than those fabricated in standard SMF (with the diameter of 125 μm) due to the reduced size of fiber cladding [19–21], which implies that SDSMF-LPG has remarkable potential to develop high-performance fiber-optic biosensors for e.g. on-chip integration.

3.2 $(PEI/PAA)_9(PEI/GOD)_1$ multilayer sensing film preparation

$(PEI/PAA)_n(PEI/GOD)_1$ multilayer film was deposited via a LbL technique, as shown shown in Fig. 3(a), and then measured by a surface profilometer. It can be seen from Fig. 3(b) that the $(PEI/PAA)_n$ multilayers display an exponential thickness growth with layer numbers [22,23]. On the other hand, the active GOD layer is very thin (about 22 nm) due to the low concentration of GOD used in the film preparation. Thin active GOD layer is useful for the solution fast diffusing into, to achieve fast response. The morphologies of the multilayer sensing films were characterized by AFM, as shown in the inset of Fig. 3(b) (more details are shown in Fig. 8, Appendix 1). The AFM images showed that the sensing film was well deposited by the LbL electrostatic self-assembly technique [22].

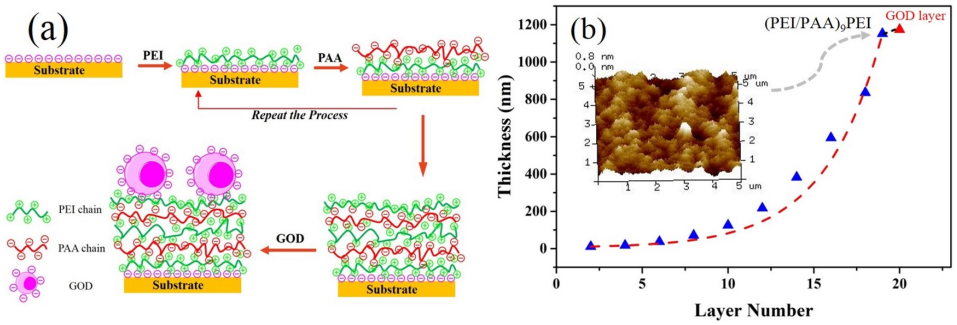

Fig. 3. (a) The layer-by-layer self-assembly scheme for the preparation of multilayer sensing film; (b) Thickness growth of the $(PEI/PAA)_9(PEI/GOD)_1$ multilayer film. The inset shows the AFM image of $(PEI/PAA)_9PEI$ multilayer film.

#259792 Received 22 Feb 2016; revised 27 Mar 2016; accepted 27 Mar 2016; published 28 Apr 2016

The spectra of the SDSMF-LPGs were measured by using a broadband light source and an optical spectra analyzer (OSA). Figure 4 shows the measured transmission spectra of the SDSMF-LPG sensor before and after deposition of $(PEI/PAA)_9(PEI/GOD)_1$ multilayer film, respectively. It can be seen that the spectral dips appear blue shift after deposition of sensing films. The result agrees with the data shown in Fig. 2 that the higher RI of multilayer sensing film induces a blue shift of the sensor's spectral dip. The shift of spectral dip indicates that the multilayer sensing film has been successfully deposited on the surface of SDSMF-LPG [24].

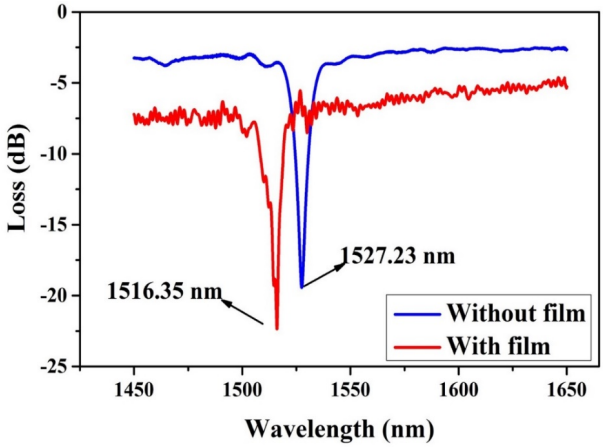

Fig. 4. Transmission spectra of the SDSMF-LPG sensor before and after depositing the sensing film.

3.3 SDSMF-LPG glucose biosensors

The sensing mechanism of the glucose biosensor is shown in Fig. 1(b). When the glucose is oxidized with the GOD catalyst, gluconic acid will be produced, and the pH of mixture solution changes with it [25]. Since the swelling degree of the $(PEI/PAA)_n$ multilayer sensing film depends on the pH of surrounding medium, the sensing film will swell with glucose concentration increasing and the induced RI change leads to a spectra shift of the SDSMF-LPG sensor [26].

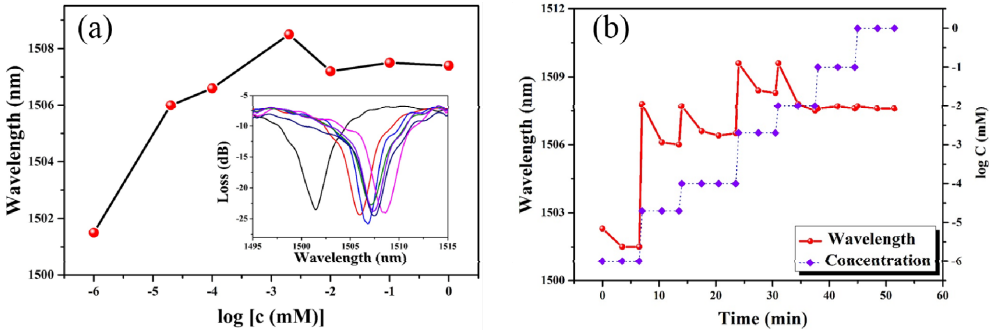

Fig. 5. (a) Response of the SDSMF-LPG biosensor to different glucose concentrations. The inset shows the measured transmission spectra; (b) the measured dynamic response of the biosensor.

The fabricated SDSMF-LPG gluocose biosensors were tested in glucose solutions with different concentrations. Figure 5(a) shows the response of the SDSMF-LPG glucose biosensor (with $(PEI/PAA)_9(PEI/GOD)_1$ multilayer film) to different glucose concentrations. It can be seen that the resonant wavelength shifts to longer values when the concentration of glucose increases. It is because the reaction product (i.e. gluconic acid) decreases the pH of

#259792 Received 22 Feb 2016; revised 27 Mar 2016; accepted 27 Mar 2016; published 28 Apr 2016

solution. As a result, more -COO^- groups are pronated to –COOH in the PAA layer and more positive charges appear on the PEI chains. Consequently, the complexation between PEI and PAA becomes weaker and the swelling degree of PEI/PAA multilayer film increases. Therefore, the RI of the sensing film will decrease, which thus induces a red shift of the spectral dip of the biosensor [27]. The spectral dip stops red shift when the glucose concentration increases to 2 μM. It is mainly because that the pH no longer changes after reacting for a specific period of time.

The dynamic response of the LPG glucose biosensor is shown in Fig. 5(b). One can see that the response time of biosensor is around 6 min. Moreover, the detection limit of the biosensor is 1 nM. It can also be seen the wavelength shifts about 5 nm when the glucose concentration changing from 1 nM to 20 nM. As the resolution of OSA is 0.02 nm, it reveals the fabricated LPG sensor can resolve the glucose change as low as 1 nM.

3.4 Fabrication and tests of the microfluidic chip

The SDSMF-LPG glucose biosensor with $(PEI/PAA)_9(PEI/GOD)_1$ multilayer film was integrated into the microchannel of a PDMS chip for microfluidic glucose sensing. As shown in Fig. 1(a), two fiber-optic glucose biosensors can be integrated into the chip for dual-parameter microfluidic sensing. A spiral microfluidic mixer is employed to mix the solutions homogeneously before passing through the two LPG sensors. It was reported that such a pre-mixing process can dramatically improve the performance of sensors [28,29].

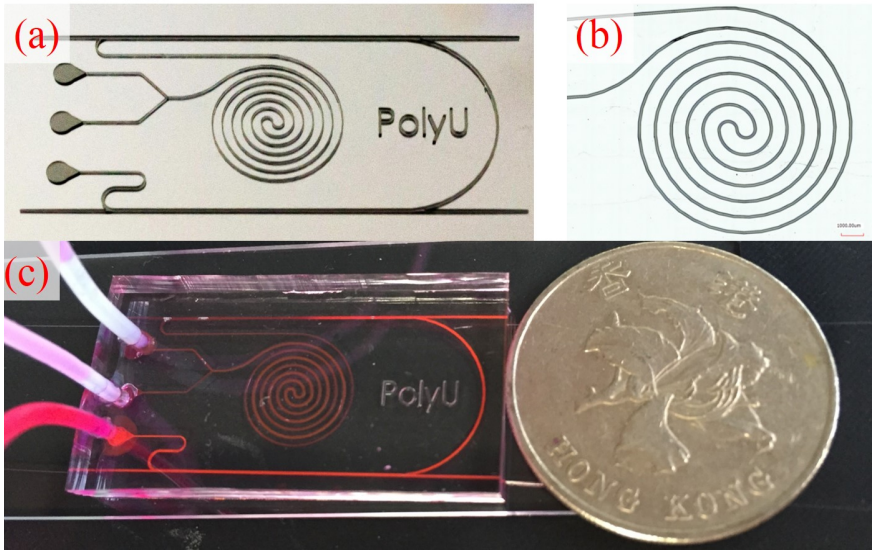

Fig. 6. Photos of the SU-8 master mould for microfluidic chip fabrication (a) and its mixer part (b); the photo of real microfluidic chip fabricated by casting PDMS on the SU-8 mould and then sealed with glass slide by using O_2 plasma (c).

Figure 6(a) shows a photo (taken by using a camera) of the SU-8 master of the microfluidic chip fabricated on the silicon substrate. An enlarge image (taken by laser scanning confocal microscope) of the spiral mixer is given in Fig. 6(b). The width and depth of the microchannel are about 110 and 260 μm, respectively (a detailed profile and size information are presented in Fig. 9, Appendix 2). It can be seen that the spiral microstructure is very uniform and its surface is pretty smooth. With the SU-8 master, a PDMS microfluidic chip was fabricated by using the moulding method. The SDSMF-LPG glucose biosensor was embedded into the chip before bonding the PDMS microfluidic chip on the glass substrate. Figure 6(c) shows the fabricated PDMS microfluidic chip integrated with the LPG glucose biosensor. The size of the microfluidic chip is small, which can thus reduce solution consumption greatly.

#259792 Received 22 Feb 2016; revised 27 Mar 2016; accepted 27 Mar 2016; published 28 Apr 2016

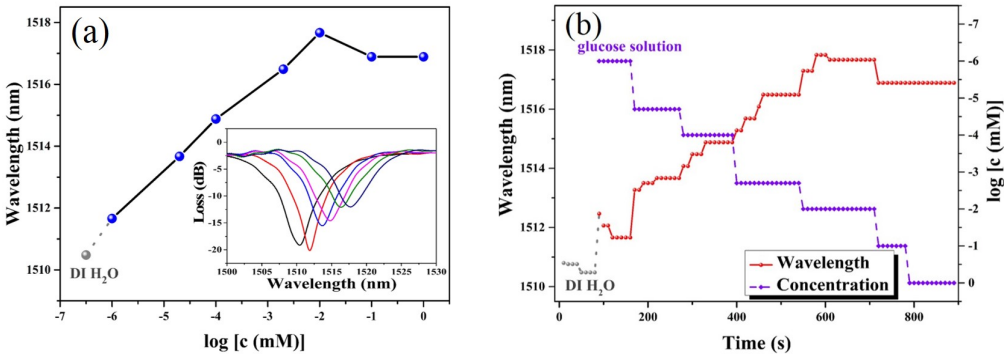

Fig. 7. (a) Response of the microfluidic chip to different glucose concentrations. The inset shows the measured transmission spectra; (b) the measured dynamic response of the glucose microfluidic chip.

The response of the microfluidic chip was tested through injecting glucose solution at the flow rate of 5 uL/min. Figure 7(a) shows the measured spectral response of the chip to different glucose concentrations. Experimental results show that the sensitivity of the microfluidic chip is very close to that of the LPG glucose biosensor measured outside of the chip, whereas the detection range is extended from 2 μM to 10 μM. The dynamic response of the microfluidic chip is presented in Fig. 7(b). One can see that the microfluidic chip can distinctly sense tiny glucose concentration as low as 1 nM. Meanwhile, the response time of the microfluidic chip was dramatically shortened from 6 minutes to 70 seconds. It can be explained that the dramatic reduction of the volume of glucose used in the test can give rise to a fast reaction between glucose and GOD layer. Therefore, the sensing film can also achieve a quick equilibrium of swelling/deswelling according to the induced pH change of the solution. The test has been repeated three times to show the repeatability of the sensor in the microfluidic chip (the detailed experimental data are presented in Fig. 10, Appendix 3). The preliminary testing results reveal that the deviation of measurement results are relatively small, which is in conformity to the robust electrostatical absorption of GOD in the sensing film.

Although the GOD can selectively catalyze the oxidization reaction of glucose solution [30], the sensor is also sensitive to the change of pH (e.g. acid substances) as its sensing film has adopted PEI/PAA multilayer for signal enhancement. One potential solution to solve this issue is to integrate one more LPG sensor, as shown in Fig. 1(a), to simultaneously monitor both pH and glucose concentration. The optical fiber pH sensor can be fabricated by using e.g. PEI/PAA multilayer [31]. Nevertheless, the demonstrated microfluidic chip has shown its remarkable performances such as ultrahigh sensitivity, fast response, and low consumption, and thus is promising to e.g. solve coagulation problem in practical clinical diagnosis [32].

4. Conclusion

A highly sensitive glucose microfluidic chip integrated with specialty optical fiber LPG sensor (inscribed in a small-diameter single-mode fiber) has been demonstrated. A layer-by-layer self-assembly technique has been successfully applied to prepare PEI/PAA multilayers on the surface of the LPG sensor. The negatively charged GOD layer was then immobilized on the multilayer film for glucose sensing. The SDSMF-LPG glucose biosensor has been eventually integrated into a PDMS microfluidic chip for glucose detection. Experimental results have revealed that such a microfluidic chip has not only an ultralow detection limit (1 nM) but also a remarkably fast response time (70 s). It is believed that such an optical fiber glucose biosensor integrated microfluidic chip has great potential for both healthcare and clinical diagnosis.

#259792 Received 22 Feb 2016; revised 27 Mar 2016; accepted 27 Mar 2016; published 28 Apr 2016

Appendix 1: AFM images of the sensing film

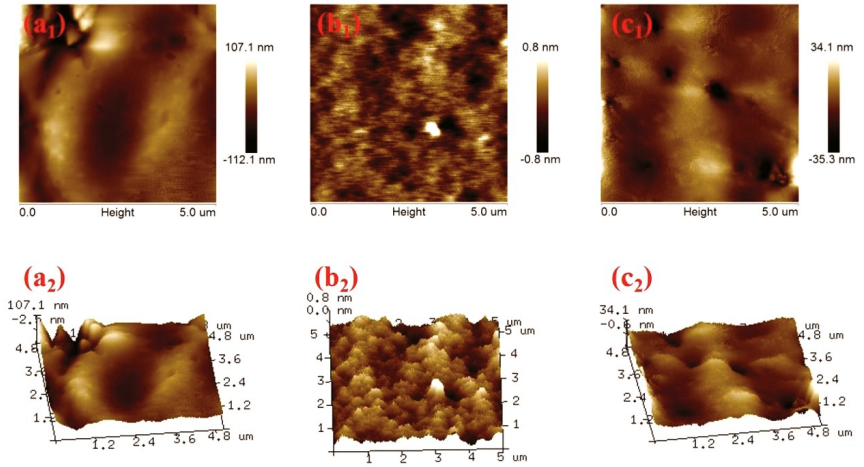

Fig. 8. AFM images of $(PEI/PAA)_9$ (a), $(PEI/PAA)_9PEI$ (b) and $(PEI/PAA)_9(PEI/GOD)_1$ (c) multilayer films: the top images are the surface morphologies and the bottom images are their 3D presentations.

Appendix 2: Images and profile parameters of the SU-8 mold for the spiral mixer

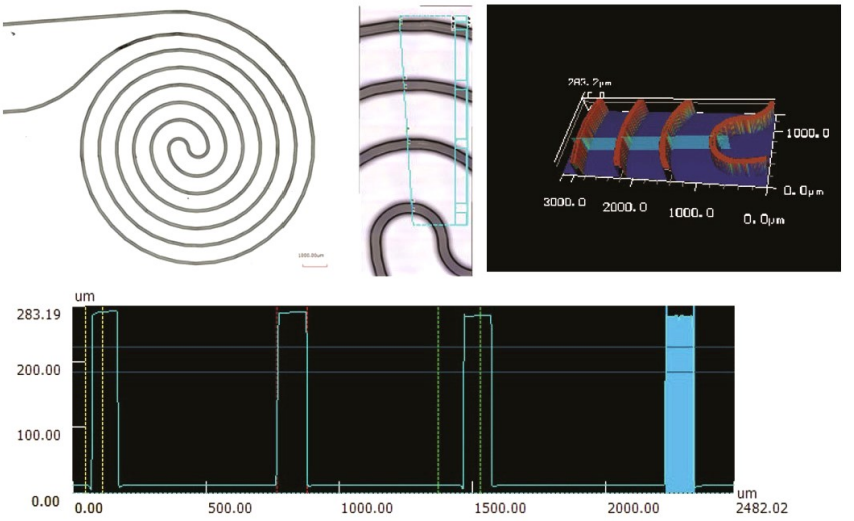

Profile1	Horz. dist.	Hght. diff.	Hght. ave.	Angle	C.S. length	C.S. area
All	2482.02um	0.51um	55.73um	0.01°	4550.72um	138388.33um2
Seg.1	63.56um	263.11um	164.17um	76.42°	327.88um	10704.71um2
Seg.2	110.39um	206.28um	263.06um	61.85°	358.05um	29197.30um2
Seg.3	160.56um	256.28um	108.03um	57.93°	425.33um	17386.08um2
Seg.4	103.70um	37.74um	265.64um	20.00°	238.68um	28009.59um2

Fig. 9. Laser scanning confocal microscopy images and profile parameters of the SU-8 mold for the spiral mixer in the microfluidic chip.

#259792 Received 22 Feb 2016; revised 27 Mar 2016; accepted 27 Mar 2016; published 28 Apr 2016

Appendix 3: Testing results and deviation analysis

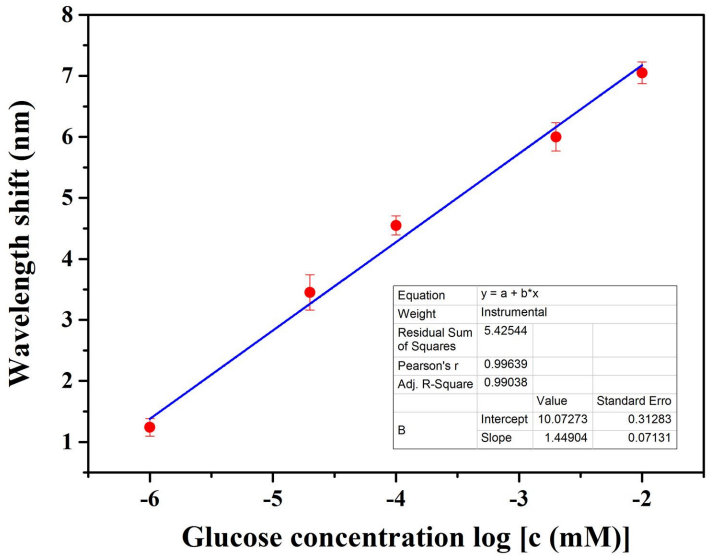

Fig. 10. Experimental results and deviation analysis of the spectral responses of the LPG biosensor integrated microfluidic chip to the change of glucose concentrations in three tests.

Acknowledgements

This work was partially supported by PolyU Gneral Research Fund (Grant No.: 1-ZVHB) and the Joint Supervision Scheme with the Chinese Mainland, Taiwan and Macao Universities (Project No.: G-SB05).